Scripta Materialia 225 (2023) 115159

Contents lists available at ScienceDirect

Scripta Materialia

journal homepage: www.journals.elsevier.com/scripta-materialia

On the reliability of using reverse Monte Carlo simulations to construct the atomic structure model of metallic glasses

Chang Liu, Zhen Zhang *, Jun Ding *, En Ma

Center for Alloy Innovation and Design (CAID), State Key Laboratory for Mechanical Behavior of Materials, Xi'an Jiaotong University, Xi'an 710049, China

ARTICLE INFO

Keywords:
Metallic glasses
Reverse Monte Carlo
Molecular dynamics
Atomic structure

ABSTRACT

Reverse Monte Carlo (RMC) simulations have been widely utilized to generate three-dimensional structural models for amorphous materials. One practical case is the modeling of atomic-level structure in metallic glasses, based on, for example, X-ray scattering and extended x-ray absorption fine structure (EXAFS) data. However, to what extent this approach can faithfully mimic the atomic structure of real metallic glasses has not been quantitatively evaluated. Using the "known" configurations from molecular dynamics simulations as the benchmark, we evaluate the reliability of RMC modeling with the total structure factor and EXAFS as the input for RMC fitting. The results indicate that the RMC-generated configuration lacks accuracy in reconstructing the local atomic packing, which tends towards the most random (and thus more energetically unfavored) state that can reproduce the reference data. To help guide towards a physically stable and meaningful atomic configuration, we advise the incorporation of additional constraints and validation check points.

Accurate three-dimensional (3D) structure models are essential for understanding the properties of disordered materials, such as liquids and glasses [1–7]. However, it has proven to be difficult to acquire detailed information of atomic arrangements in amorphous materials via traditional experimental methods. Typical experimental techniques such as X-ray diffraction (XRD) or neutron scattering measurements usually give only angular-averaged structural information, which could correspond to a vast variety of 3D arrangement of atoms. Other difficulties facing experimental measurements including the resolution of partial pair correlations and the short-range chemical order in muti-component systems. For the latter, extended X-ray absorption fine structure (EXAFS) experiments were shown to provide some insights [5,8], but still far from offering a complete picture. To complement the structural information attainable from experimental measurements, computer simulations have proven to be valuable tools which allow to resolve atomic-level structure of glass systems. However, the reliability of the commonly employed simulation methods, i.e., classical molecular dynamics relies on a faithful description of the interactions between constituent atoms, which is still a challenging task since classic potentials usually have a limited accuracy, while *ab initio* potential calculations are computationally very demanding [9,10].

To circumvent these difficulties as mentioned above, reverse Monte Carlo (RMC) technique [11] has been used for modeling the structure of liquids and glasses, without knowing *a priori* the interatomic potentials. RMC approach usually takes a sort of experimentally measured structural quantities of an amorphous material as inputs for fitting a structural model which then allows for further analysis of the atomic arrangements. For metallic glasses (MGs), Sheng et al. [5] and Luo et al. [12] have successfully employed RMC modeling based on experimental structure information of XRD and EXAFS to resolve their atomic configuration and elucidated the nature of the short-range order (SRO) such as dominant Frank-Kasper polyhedra, and medium-range order (MRO) (i.e., solute-centered quasi-equivalent cluster packing). The combination of XRD and EXAFS were selected because those two experimental characterizations are highly complementary in illustrating the atomic packing of MGs: specifically, the former is essentially a condensation of angular averaged structural information over a wide length scale, while the latter is a probe of species-specific local coordination information [4]. Furthermore, such RMC approach has been also applied on MGs with a series of compositions and revealed the correlation between atomic packing efficiency and glass forming ability [13]. However, it has been long-term questioned on the validity and accuracy of RMC-reconstructed configuration for complex amorphous materials, by simply fitting the diffraction data such as structure factor or radial distribution function, and/or EXAFS spectra [11,14,15]. Due to the unknown structural details of experimental MG samples, there is still a

* Corresponding authors.
E-mail addresses: zhen.zhang@xjtu.edu.cn (Z. Zhang), dingsn@xjtu.edu.cn (J. Ding).

https://doi.org/10.1016/j.scriptamat.2022.115159
Received 27 September 2022; Received in revised form 29 October 2022; Accepted 5 November 2022

lack of understanding about to what extent the RMC-generated structure can reliably describe the atomic structure, in particular their local atomic environments [4], by combining XRD and EXAFS information.

In this work, we aim to quantitatively evaluate the reliability of the RMC modeling approach based the simulated XRD and EXAFS spectra as typically utilized in experiments. The materials under consideration are three representative MGs, namely amorphous Ta, $Cu_{50}Zr_{50}$ and $Cu_{64}Zr_{36}$. This selection of alloy compositions is of practical relevance and allows us to discuss the role of composition complexity in the performance of RMC modeling. The glass configurations generated by classical MD simulations are treated as target structures from which the input structural parameters are extracted. The reconstructed structures from the RMC simulations are then compared with the target structures to assess in a quantitative manner the reliability of the RMC modeling in predicting the atomic structure of the MGs.

The target structures of the amorphous Ta, $Cu_{50}Zr_{50}$ and $Cu_{64}Zr_{36}$ MGs were produced by classical MD simulations using a melt-quench procedure. The simulations were performed using the LAMMPS code [16] and the embedded atom method (EAM) potentials from Refs. [17, 18] were used for describing the interatomic interactions. The simulation boxes contain 16,000 and 10,000 atoms for Ta and Cu-Zr, respectively, and the initial box sizes were determined by the corresponding glass densities. These samples were first melted at 4000 K, and 2500 K for Ta and Cu-Zr, respectively for 100 ns, a time span that is sufficient to equilibrate the melts. The glass samples were obtained by quenching the equilibrated melts down to 300 K with a constant cooling rate of 10^{14} K/s for Ta and 10^{10} K/s for Cu-Zr. These MD-simulated MG configurations were used as target for the RMC modeling. All MD simulations were carried out in the isothermal–isobaric ensemble under zero pressure and using a time step of 2 fs.

We have considered two practical structure quantities as inputs for RMC simulation, namely the total X-ray structure factor and EXAFS. X-ray structure factor is a widely used technique for structural analysis, which is often diffuse, with a wide first diffraction maximum, and several others that damp and diminish quickly for MGs [19,20]. Meanwhile, EXAFS is the normalized description of X-ray absorption spectrum, whose oscillations are sensitive to short-range local environment [21,22]. The inverse Fourier-transformed EXAFS spectra, which is used as input for RMC modeling, was calculated using the FEFF software [23]. Local atomic packing was studied using the Voronoi tessellation method [24,25].

RMC simulations, based on the total structure factor and the EXAFS spectra calculated from the target MD-generated structure, was employed to reconstruct 3D atomic configuration of the corresponding MGs. The RMC modeled systems were assigned with the same number of atoms and the same densities as the target configurations. The protocol of our RMC simulation proceeds through the following iteration: (1) Generate a new configuration by randomly displacing atoms in the simulation box; (2) Calculate the normalized fit residue between the structure parameters from the trial configuration and the target configuration, which is written as [12,26]:

$$\chi^2_{fit} = \sum \frac{\delta^2}{\sigma^2} = \sum_i \left\{ \frac{\left|\Omega^i_{trial} - \Omega^i_{target}\right|^2}{\left|\Omega^i_{target}\right|^2 \sigma_i^2} \right\} \tag{1}$$

In this expression, δ^2 and σ^2 can be viewed as the "energy" term and the "temperature" term in MD simulations; The term i indicate the structural quantities of MGs, e.g., X-ray structure factor, and EXAFS for each constituting element; 3) Compare the fit residue of the current guess configuration with the one in the previous cycle χ^2_0, accept the new move if $\chi^2_{fit}<\chi^2_0$. Otherwise, the move is accepted with the probability $\exp\left(\frac{\chi^2_0-\chi^2_{fit}}{2}\right)$ (i.e., via the metropolis algorithm) [26]. While repeating the above iteration, σ has been gradually reduced from 0.1 to 10^{-3} for structure factor and from 10^{-4} to 10^{-6} for EXAFS, to mimic the quenching process in the MD simulations. The above procedure is continued until the "energy'' term δ^2 is minimized via RMC++ software [27]. The whole procedure is schematically illustrated in Fig. 1. We have found that the RMC-reconstructed configurations starting from different random initial configurations exhibit the same level of quality in matching the various properties of the target structure. Hence, we present in the following the results of one RMC configuration for each composition.

To begin with, Fig. 2 shows that the structural models obtained from the RMC simulations excellently reproduce (with R^2>0.99) the X-ray structure factor, $S(q)$, and EXAFS of the target MD structures. $S(q)$ can be calculated by the expression:

$$S(q) = \sum_\alpha \sum_\beta \frac{c_\alpha c_\beta f_\alpha f_\beta}{\left(\sum_\alpha c_\alpha f_\alpha\right)^2} S_{\alpha\beta}(q) \tag{2}$$

where c_α and c_β are respectively the molar fractions of species α and β, f_α and f_β are the corresponding atomic scattering factors [19,20], and the partial structure factor $S_{\alpha\beta}(q)$ is given by [19]:

$$S_{\alpha\beta}(q) - 1 = \frac{4\pi\rho}{q} \int_0^\infty r\left[g_{\alpha\beta}(r) - 1\right] \sin(qr) dr \tag{3}$$

where r is the inter-atomic distance, $g_{\alpha\beta}(r)$ is the partial radial distribution function (RDF) for the atomic pair between element α and β [19]. The EXAFS at the absorption edge of element α with multiple components is written as [21,22]:

$$\chi_\alpha(k) = \sum_\beta S_{0\beta}^2 \frac{|f(k)|}{k} 4\pi\rho \frac{N_\beta}{N} \int g_{\alpha\beta}(r) \sin(2kr + 2\delta_c + \phi) e^{-2r/\lambda(k)} dr \tag{4}$$

where S_0 is the overall amplitude, $|f(k)|$ is the back-scattering amplitude, N_β is the coordinated atomic number of element β for element α, δ_c is central-atom partial-wave phase shift of the final state, ϕ is phase shift, and $\lambda(k)$ is the energy-dependent EXAFS mean free path. EXAFS is usually presented as a function of the wave number of photo-electron k and multiplied by a power of k typically k^2 or k^3 to emphasize the oscillations [21,22].

These results in Fig. 2 are as expected since these two structural quantities were used as input for the RMC modeling. The fact that the goodness-of-fit remains in a high level for the three MGs indicates that the applied fitting strategy works well despite compositional complexity. However, as we have mentioned earlier, a more stringent test of the reliability of the RMC-generated atomic configuration is through comparison of the structural quantities that are *a priori* unknown for the RMC modeling. In the following, we will present several representative structural quantities to give a more comprehensive evaluation of the structure similarity between the target and RMC-

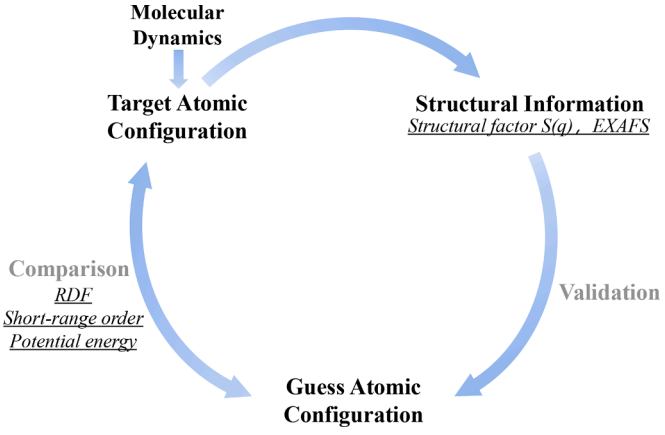

Fig. 1. Sketch of the simulations and evaluation of the RMC modeling.

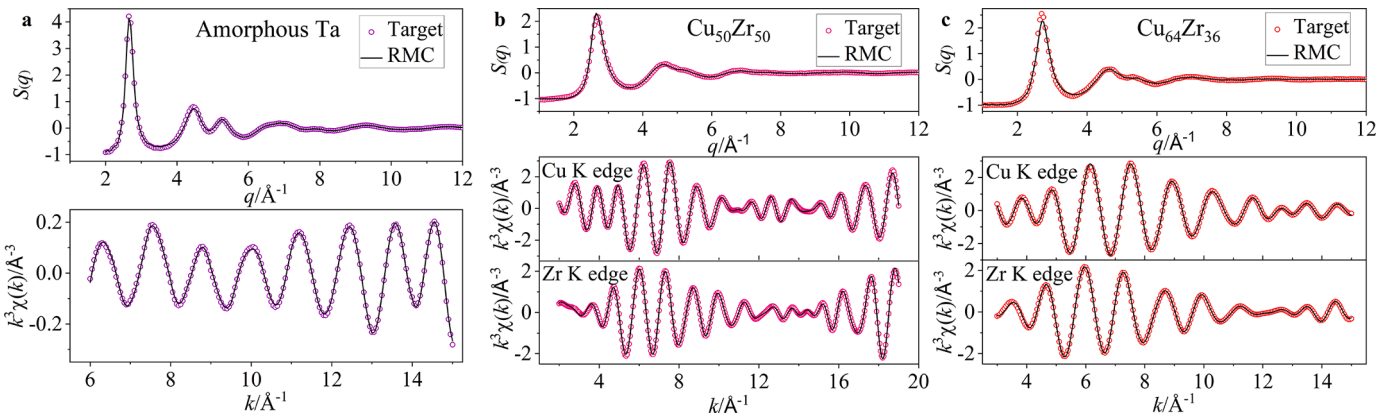

Fig. 2. Comparison of the total *S(q)* and EXAFS spectra obtained from the target and RMC-reconstructed configurations. (a) to (c) are for the Ta, $Cu_{50}Zr_{50}$ and $Cu_{64}Zr_{36}$ MGs, respectively.

reconstructed atomic configurations.

Fig. 3 compares the RDFs of the target structure with the RMC-reconstructed structure from RMC modeling. Overall, the total RDF of the guess configuration is in good agreement with that of the target structure (R^2>0.99), which could be attributed to the fact that the total RDF is essentially the real space version of *S*(*q*). Stronger deviation of the guess structure from the target structure is seen in the partial RDFs, panels (b) and (c). This result indicates that although the inclusion EXAFS data in the fitting can provide some information regarding short-range chemical ordering, it is still insufficient to allow a full account of the 3D atomic arrangement. The degree of this insufficiency does not seem to be influenced by the deviation of the constituting atomic species from equal proportion, see panels (b)-(c), as evidenced by the fact that the R^2 values of the partial RDFs of $Cu_{64}Zr_{36}$ are nearly the same as these of $Cu_{50}Zr_{50}$. Besides, other RDF-related quantities, such as bond angle distribution and the coordination environment of the atoms are also expected to exhibit discrepancies between the guess and the target structure. Here, the local atomic packing of the atoms is of particular interest and thus will be presented next.

The Voronoi tessellation method has been employed to characterize the local atomic environment. Fig. 4 shows that the fractions of various coordination polyhedra are different between the reconstructed and the target atomic configurations and that this structural discrepancy is already quite pronounced in the monoatomic amorphous Ta, panel (a). Overall, we note that the reconstructed atomic configurations show a weaker icosahedral SRO and five-fold symmetry due to the lower average coordination numbers and decreasing occurrences of clusters with high fractions of five-fold bonds such as ⟨0,0,12,0⟩, ⟨0,1,10,2⟩, ⟨0,2,8,1⟩ and ⟨0,2,8,2⟩ clusters. This is accompanied by the increase of other distorted structures such as ⟨0,3,6,4⟩ for Ta, ⟨0,3,6,2⟩ for $Zr_{50}Cu_{50}$ and $Zr_{36}Cu_{64}$, indicating an increasing disclination density [4]. (Note that only the Voronoi polyhedra with the highest fractions in the target structure are shown in the graph). The weaker icosahedral SRO and five-fold symmetry, increasing disclination density, and a broader distribution of Voronoi polyhedra substantiate that the reconstructed structure by RMC modeling is more disordered than the target structure, which is consistent with the fact that RMC favors maximal randomness [4].

In addition to the evaluation of structural features, potential energy is introduced as an overall measure of the stability of the obtained 3D structure models. As shown in Fig. 5, the potential energy of RMC-reconstructed atomic configurations are much higher than that of the corresponding "real" atomic configurations, and the former configuration should not even remain stable at room temperature. This result is in accordance with the nature of the RMC method itself because among all possible configurations that matches the target structure information, RMC modeling tends to select the most random (unstable) one with the highest entropy [28]. Such result can also be related to the short-range ordering of the MG structure: The icosahedral structure along with its five-fold symmetry behave as a stabilizer in amorphous alloys [4] and thus the decrease of their concentrations in the guess atomic configurations relative to the target structures is the structural origin of their higher potential energies. Finally, we note that the observed high energy state of the guess structure relative to the target structure is independent of the compositional complexity.

Based on the results presented above, the deficiency of the RMC modeling becomes evident: While the guess structures reproduce very well the total structure factor and EXAFS spectra used for the RMC

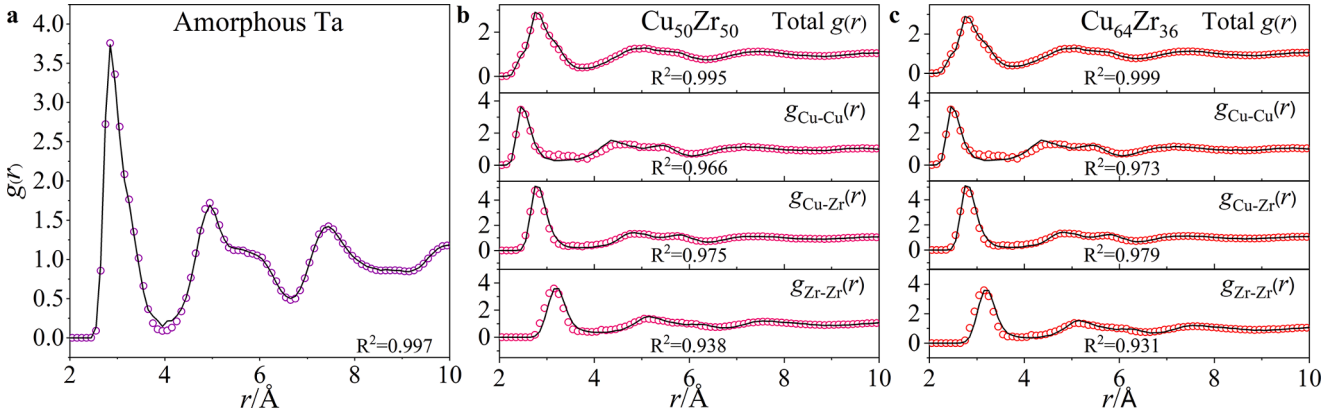

Fig. 3. Comparison of the RDFs obtained from the target (circles) and RMC-reconstructed atomic configurations (black lines). (a) to (c) are for the Ta, $Cu_{50}Zr_{50}$ and $Cu_{64}Zr_{36}$ MGs, respectively.

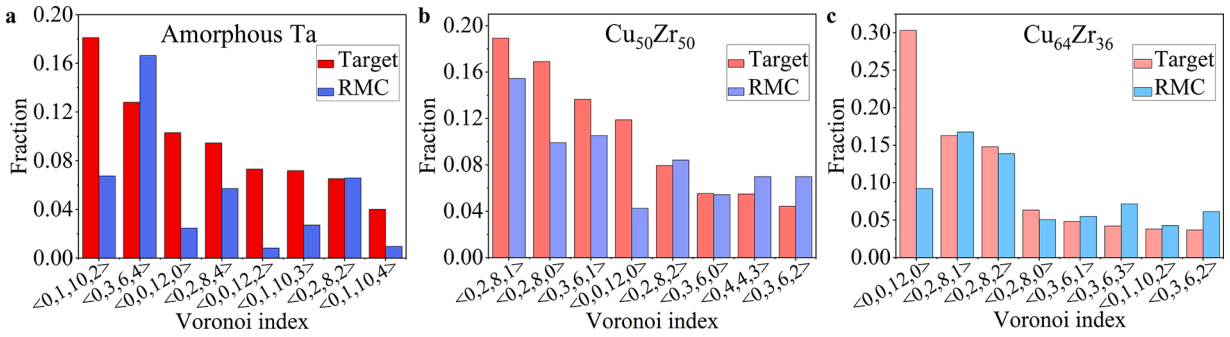

Fig. 4. Comparison of the fractions of various coordination polyhedra (with different Voronoi indices) between the RMC-reconstructed atomic configurations and the target atomic configurations. (a) to (c) are for the Ta, $Cu_{50}Zr_{50}$ and $Cu_{64}Zr_{36}$ MGs, respectively. In panels (b) and (c), the Voronoi polyhedra are Cu centered.

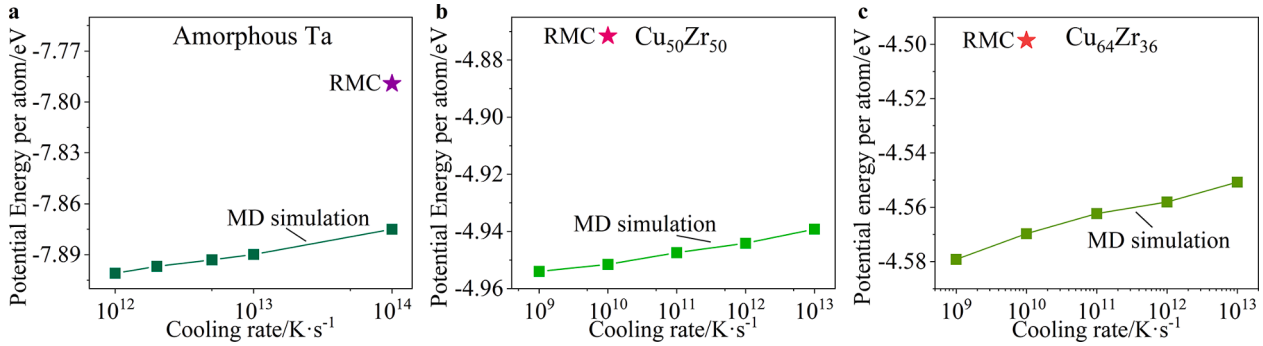

Fig. 5. Comparison of potential energies between the RMC-reconstructed atomic configurations produced by RMC modeling and the target configurations produced by MD simulations. (a) to (c) are for the Ta, $Cu_{50}Zr_{50}$ and $Cu_{64}Zr_{36}$ MGs, respectively.

fitting, they are not able to give a reliable description of the element-specific structures, notably the short-range order. This finding thus casts doubts on the reliability of the RMC modeling results from previous studies which typically adopt experimentally measured XRD and EXAFS spectra as input for the fitting. We note that the reasons for this deficiency are two folds: (1) The inputs for the RMC simulation, i.e., total structure factor and EXAFS spectra, do not allow for a full account of the atomic arrangements in the target structure which are rather complex in amorphous materials; (2) RMC samples the configurational space in a random manner, and thus the final configuration is essentially the most random structure that can reproduce the target structural parameters. That being said, if the constraints (i.e., inputs for RMC modeling) are not strong enough, the system may conceivably end up in a state with unrealistically high energy, because interatomic interactions are not considered during the RMC fitting.

Clearly, further optimization of the RMC modeling is required in order to achieve accurate description of the atomic structure of MGs. First, for systems containing more than one element, one may need to at least include the partial RDFs [29] or equivalent information in RMC fitting as already been tested in a previous study [8] which has reported an increased accuracy of the RMC modeling in reproducing the short-to-medium range structures of a MG. In addition to the partials, it is also feasible to introduce additional structural information as constraints such as fluctuation electron microscopy (FEM) [30,31] and 4D STEM [32,33], which can provide more details on the atomic arrangements at larger length scales. A further constraint that one can apply to RMC modeling is the "potential energy" term since energy is a more sensitive and comprehensive representation of the structural order. The energy term can effectively narrow the range of possible atomic configurations that match with the input structural information by requiring that the reconstructed structure is also thermodynamically favored among others. The potential energy can be evaluated using classical interaction potentials or machine learning potential [34,35] that are becoming increasingly prevalent. We note that this energy constraint only has to be applied at a fraction of the RMC steps, thus avoiding the time-consuming calculation of energies at every step in MD simulations.

The reliability of RMC modeling in reproducing the 3D atomic structure of "known" MD-generated glass configurations has been quantitatively evaluated. We have found that the total XRD structure factor and the EXAFS spectra as inputs for the RMC simulations allow for a satisfactory reproduction of the total structural quantities, such as the total RDF, and even the partial RDFs (but to a less degree of satisfaction). Strong discrepancies were observed for the local atomic environments between the atoms in the target structure and RMC-reconstructed structure, thus indicating the limitation of the popularly applied RMC modeling approach in giving an accurate description of the local structural order. The inclusion of more/independent constraints, such as the partial RDFs, the 3D structural information as encoded in the FEM or 4D-STEM, and the potential energy term are expected to further improve the reliability of RMC-generated structure models.

CRediT authorship contribution statement

Chang Liu: Methodology, Data curation, Writing – original draft. **Zhen Zhang:** Data curation, Formal analysis, Investigation, Writing – review & editing. **Jun Ding:** Conceptualization, Data curation, Supervision, Writing – review & editing. **En Ma:** Conceptualization, Writing – review & editing.

Declaration of Competing Interest

The authors declare no competing interests. The authors declare that they have no known competing financial interests or personal relationships that could have appeared to influence the work reported in this paper.

Acknowledgment

J.D., Z.Z. and E.M. thank Xi'an Jiaotong University for supporting their work at the Center for Alloy Innovation and Design (CAID). J.D. acknowledges support from National Natural Science Foundation of China (12004294), National Youth Talents Program and the HPC platform of Xi'an Jiaotong University.

References

[1] J.P. Hansen, I.R. McDonald, Theory of Simple Liquids, Academic Press (1990).
[2] S.R. Elliott, Medium-range structural order in covalent amorphous solids, Nature 354 (1991) 445–452.
[3] D.B. Miracle, A structural model for metallic glasses, Nat. Mater. 3 (2004) 697–702.
[4] Y.Q. Cheng, E. Ma, Atomic-level structure and structure-property relationship in metallic glasses, Prog. Mater Sci. 56 (4) (2011) 379–473.
[5] H.W. Sheng, et al., Atomic packing and short-to-medium-range order in metallic glasses, Nature 439 (7075) (2006) 419–425.
[6] H. Tanaka, et al., Revealing key structural features hidden in liquids and glasses, Nat. Rev. Phys. 1 (5) (2019) 333–348.
[7] Z. Zhang, W. Kob, Revealing the three-dimensional structure of liquids using four-point correlation functions, PNAS 117 (25) (2020) 14032–14037.
[8] W.K. Luo, E. Ma, EXAFS measurements and reverse Monte Carlo modeling of atomic structure in amorphous $Ni_{80}P_{20}$ alloys, J. Non Cryst. Solids 354 (10–11) (2008) 945–955.
[9] R. Car, M. Parrinello, Unified approach for molecular dynamics and density-functional theory, Phys. Rev. Lett. 55 (22) (1985) 2471–2474.
[10] G. Kresse, J. Hafner, Ab initio molecular dynamics for liquid metals, Phys. Rev. B 47 (1) (1993) 558–561.
[11] R.L. McGreevy, L. Pusztai, Reverse Monte Carlo simulation: a new technique for the determination of disordered structures, Mol. Simul. 1 (6) (1988) 359–367.
[12] W.K. Luo, et al., Icosahedral short-range order in amorphous alloys, Phys. Rev. Lett. 92 (14) (2004), 145502.
[13] L. Yang, et al., Atomic-scale mechanisms of the glass-forming ability in metallic glasses, Phys. Rev. Lett. 109 (2012), 105502.
[14] M.I. Mendelev, M.J. Kramer, Reliability of methods of computer simulation of structure of amorphous alloys, J. Appl. Phys. 107 (7) (2010), 073505.
[15] X.W. Fang, et al., Structure of $Cu_{64.5}Zr_{35.5}$ metallic glass by reverse Monte Carlo simulations, J. Appl. Phys. 115 (5) (2014).
[16] A.P. Thompson, et al., LAMMPS - a flexible simulation tool for particle-based materials modeling at the atomic, meso, and continuum scales, Comp. Phys. Comm. 271 (2022) 10817.
[17] Y.Q. Cheng, E. Ma, H.W. Sheng, Atomic level structure in multicomponent bulk metallic glass, Phys. Rev. Lett. 102 (24) (2009), 245501.
[18] L. Zhong, J.W. Wang, H.W. Sheng, Z. Zhang, S.X. Mao, Formation of monatomic metallic glasses through ultrafast liquid quenching, Nature 512 (2014) 177–180.
[19] T. Egami, S.J.L. Billinge, Underneath the Bragg peaks: structural analysis of complex materials, editor, in: RW Cahn (Ed.), Pergamon Materials Series, Elsevier, Oxford, 2003. vol. 7.
[20] T.C. Hufnagel, X.F. Gu, A. Munkholm, Anomalous small-angle X-ray scattering studies of phase separation in bulk amorphous $Zr_{52.5}Ti_5Cu_{17.9}Ni_{14.6}Al_{10}$, Mater. Trans. 42 (4) (2001) 562–564.
[21] J.J. Rehr, R.C. Albers, Theoretical approaches to X-ray absorption fine structure, Rev. Mod. Phys. 72 (3) (2000) 621–654.
[22] A.L. Ankudinov, et al., Real-space multiple-scattering calculation and interpretation of X-ray-absorption near-edge structure, Phys. Rev. B 58 (12) (1998) 7565–7576.
[23] J.J. Rehr, et al., Parameter-free calculations of X-ray spectra with FEFF9, Phys. Chem. Chem. Phys. 12 (21) (2010) 5503–5513.
[24] G. Voronoi, New parametric applications concerning the theory of quadratic forms – second announcement, J. Reine Angew. Math. 134 (1/4) (1908) 198–287.
[25] Y.Q. Cheng, J. Ding, E. Ma, Local topology vs. atomic-level stresses as a measure of disorder: correlating structural indicators for metallic glasses, Mater. Res. Lett. 1 (1) (2013) 3–12.
[26] R.L. McGreevy, Reverse Monte Carlo modelling, J. Phys. Condens. Matter 13 (46) (2001) R877–R913.
[27] O. Gereben, et al., A new Version of the RMC++ Reverse Monte Carlo Programme, Aimed at Investigating the Structure of Covalent Glasses, J Optoelectron. Adv Mater 9 (2007) 3021–3027.
[28] R.L. McGreevy, RMC: progress, problems and prospects, Nucl. Instrum. Methods. Phys. Res. A 354 (1) (1995) 1–16.
[29] L. Pusztai, G. Tóth, Simple liquids, partial radial distribution functions, J. Chem. Phys. 94 (4) (1991) 3042–3049.
[30] M.M.J. Treacy, J.M. Gibson, Variable coherence microscopy: a rich source of structural information from disordered materials, Acta Crystallogr. A 52 (1996) 212–220.
[31] J. Hwang, et al., Reverse Monte Carlo structural model for a zirconium-based metallic glass incorporating fluctuation microscopy medium-range order data, J. Mater. Res. 24 (10) (2009) 3121–3129.
[32] C. Ophus, Four-Dimensional Scanning Transmission Electron Microscopy (4D-STEM): from Scanning Nanodiffraction to Ptychography and Beyond, Microsc. Microanal. 25 (3) (2019) 563–582.
[33] T.C. Pekin, et al., Direct measurement of nanostructural change during *in situ* deformation of a bulk metallic glass, Nat. Commun. 10 (2019) 2445.
[34] T. Mueller, A. Hernandez, C.H. Wang, Machine learning for interatomic potential models, J. Chem. Phys. 152 (2020), 050902.
[35] T.Q. Wen, L.F. Zhang, H. Wang, E. WN, D.J. Srolovitz, Deep potentials for materials science, Mater. Futur. 1 (2) (2022), 022601.